

NATIONAL ADVISORY COMMITTEE FOR AERONAUTICS

TECHNICAL NOTE 3566

A POLAR-COORDINATE SURVEY METHOD FOR DETERMINING
JET-ENGINE COMBUSTION-CHAMBER PERFORMANCE

By Robert Friedman and Edward R. Carlson

Lewis Flight Propulsion Laboratory
Cleveland, Ohio



Washington
September 1955

RECEIVED
AFL 2016



NATIONAL ADVISORY COMMITTEE FOR AERONAUTICS

TECHNICAL NOTE 3566

A POLAR-COORDINATE SURVEY METHOD FOR DETERMINING

JET-ENGINE COMBUSTION-CHAMBER PERFORMANCE

By Robert Friedman and Edward R. Carlson

SUMMARY

The use of an automatic polar-coordinate traversing system for determining jet-engine combustor performance is described. A combined temperature and pressure probe is swept circumferentially through a quarter-annular exhaust duct at selected radial positions. Data are recorded as a function of probe position.

This method furnishes complete temperature, pressure, and flow profiles with a single probe. It provides a means of calculating mass-weighted or area-average mean temperatures and pressures for evaluating combustion efficiency and pressure loss. An example is given to illustrate these procedures.

INTRODUCTION

Jet-engine combustion-chamber design must conform to many requirements specified by carbon deposition, liner temperature, size, combustion stability, temperature profile, pressure drop, and combustion efficiency. Many of these requirements may be evaluated by inspection and simple measurements, but evaluation of the latter three characteristics entails more elaborate research instrumentation. For determination of temperature profiles, local temperatures at a combustor-exhaust plane normal to the gas flow are needed. For combustion efficiency and pressure loss, weighted mean temperatures and total pressures are required (ref. 1). Local temperatures and total pressures are commonly measured by multiple rakes of thermocouples and total-pressure tubes. Mean temperatures and mean total pressures are calculated by mass-weighting these local measurements, as shown in references 1 and 2.

The high-temperature jet-engine combustion systems now under development present additional difficulties, because accurate measurements are difficult to obtain at the high-temperature and relatively low Mach

3532

T-90

number conditions. Furthermore, because of large variations in the temperature distribution and uneven velocity distributions, an increasing number of measuring elements is required for an adequate survey (ref. 3).

These problems were resolved at the NACA Lewis laboratory by a survey method which consists of a traversing mechanism for covering the complete combustor-exhaust plane and computation techniques for obtaining representative data values from these traverses. The survey system uses a combined thermocouple and total-pressure-tube probe. The single probe, as opposed to multiple rakes, allows the use of complicated sensing elements suited to high temperatures, such as the sonic aspirated thermocouple first described in reference 4. This survey system was adapted for use in annular gas passages by means of a polar-coordinate sweep movement, which actuates the probe automatically. Temperature and pressure are recorded continuously against probe position.

This report shows the application of this survey method to the determination of temperature, pressure, and velocity profiles, combustion efficiency, and pressure loss. An example of high-temperature combustor profiles is presented to illustrate these procedures and the results of the use of the survey method in combustor performance evaluation.

SYMBOLS

A	area
ΔA	area increment
g_c	force-mass conversion factor, 32.2 lb(mass)-ft/lb(force)(sec ²)
M	Mach number
P_m	mass-weighted mean total pressure
P_t	absolute total pressure
ΔP_t	total-pressure loss across combustor
$P_{t,1}$	combustor-inlet total pressure
p	absolute static pressure
q	dynamic pressure, $\frac{1}{2} \rho V^2$
q_1	combustor-inlet dynamic pressure
R	specific gas constant

T_m	mass-weighted mean total temperature
T_t	absolute total temperature (in numerical examples given in $^{\circ}\text{F}$ rather than in absolute units)
V	velocity
w	mass-flow rate
γ	ratio of specific heats
ρ	density

DESCRIPTION OF SURVEY SYSTEM

Turbojet combustor-exhaust passages are commonly annular in shape. While previous traversing systems for these ducts have appeared in the literature (refs. 1 and 5), the survey method described herein offers a means of obtaining a more complete traverse by moving a single-point probe circumferentially across the duct passage at a number of radial stations. A polar-coordinate probe movement allows the probe to be positioned from a fixed pivot point outside the duct, simplifying the probe actuation.

Although the survey method could be adapted to a number of different flow-passage geometries, the one considered here was designed for use with a 90° sector of an annular combustor, frequently used in laboratory installations to conserve air and fuel supplies. The polar-coordinate survey section constructed at the Lewis laboratory is shown in figure 1. The probe enters the gas passage through a wall-enclosed slot below the duct. The probe is swept circumferentially by an angular drive hub, held in place by bearing blocks below the cooled duct walls, and driven radially through a shaft below the hub.

A cross-sectional view of the probe installation is shown in figure 2. The passage between the probe and the radial-drive lead screw is pressurized by outside air for cooling. This air escapes through holes drilled in the clamping collet which holds the bottom of the probe to the lead screw. Escape of the cooled air into the combustor-exhaust duct through the probe access slot is minimized by drawing the cooling air out through the vacuum connection just below the angular-drive hub. The vacuum outlet may be omitted for combustor operation at high pressures.

The probe chosen for this example consists of two elements: a total-pressure tube and a platinum-13-percent-rhodium - platinum thermocouple. The principles of the sonic-aspirated thermocouple are described in references 2, 4, and 6 to 8. This type has the advantages of constant recovery factor and negligible radiation and conduction errors (ref. 9). A vacuum connection allows the exhaust gases to be drawn through the nozzle past the thermocouple junction at sonic velocities.

3532

back T-50

A complete polar-coordinate survey of an annular passage with a single probe requires both radial and circumferential traverses. A practical, time-saving compromise is to sweep the probe circumferentially at several predetermined radii. Any number of these circumferential sweeps may be used, but for this specific application five radial positions were found to be sufficient. The path traced by the probe tip is shown in figure 3. From either of two terminal positions represented by circles, the probe moves angularly until the entire circumference is surveyed, then repositions radially for a return circumferential sweep, and so on until the five circumferential sweeps are completed. Position measurements were obtained from a potentiometer geared to the angular-drive hub. When used with an X-Y recorder, this survey method thus furnishes five circumferential data profiles. The five radii are at centers of equal annular areas.

The path shown in figure 3 is traversed automatically after the operator closes a start switch. Mechanical and electronic details of the automatic positioning control are given in appendix A.

Since this is an analog system, the response time of the measuring elements is of importance. By application of thermocouple time-constant methods, such as those of reference 10, a negligible temperature-response lag was attained by establishing a probe traverse velocity sufficiently slow with respect to the response time. In the example cited in this report, an angular traversing velocity that allowed a single circumferential sweep to be completed in 40 seconds was found to be satisfactory. Accuracy of the angular-position-transmitting potentiometer was 0.1 percent; accuracy of the radial-actuator positioning was also 0.1 percent.

Temperature, total-pressure, and angular-position indications were converted to the scale requirements of a recorder by separate matching units of precision resistors for the respective thermocouple, transducer, and position potentiometer signals. Thermocouple readings were corrected for a constant recovery factor (ref. 4). Static pressure was not determined by surveys but was measured instead from taps located in the exhaust-duct side walls.

APPLICATIONS

Profiles

Temperature and pressure profiles are obtained directly from the survey. Measurements of dynamic pressure, or the difference between total and static pressures, is preferred to the direct recording of total pressure, since in this way a sensitivity to small pressure variations at high total-pressure levels is retained. Dynamic-pressure measurements are made by connecting total- and static-pressure lines to a pressure transducer, which transmits a signal to the recorder indicative of the difference between the two pressures. For this example,

sufficiently accurate dynamic pressures were obtained from the probe total-pressure tube and a representative duct static pressure measured at the side-wall taps. Where very accurate dynamic pressures are desired, however, static pressure as well as total pressure should be surveyed.

Velocity profiles are constructed from values calculated from the temperature, static-pressure, and dynamic-pressure measurements. The appropriate equations for the calculation of velocity for both compressible and incompressible flow assumptions are given in appendix B. Mach number and mass-flow profiles are constructed from values calculated by equations also developed in appendix B.

Combustion Efficiency

Combustion efficiency is defined as the ratio of the heat energy actually developed in the gas stream to the heat energy theoretically available from complete combustion. While the increase in energy may be determined from thrust measurements (ref. 11) or exhaust-gas analyses (ref. 5), it is commonly calculated from the average combustor-exhaust temperature rise (ref. 12). This requires temperature measurements at inlet and outlet stations of the combustor. At the combustor inlet, with a uniform temperature, there are rarely any difficulties; but at the outlet, a mass-weighted temperature must be calculated (i.e., the temperature of a uniform stream having the same mass flow and the same heat energy as the actual exhaust gases). As shown in references 1 and 2, the mass-weighted temperature is expressed as

$$T_m = \frac{\int T_t dw}{\int dw} \quad (1)$$

Since the weighting is usually performed as a summation of a finite number of local values at area increments,

$$T_m = \frac{\sum T_t \left(\frac{w}{A}\right) \Delta A}{\sum \left(\frac{w}{A}\right) \Delta A} \quad (2)$$

Substituting the incompressible-flow relations for mass flow derived in appendix B gives

$$T_m = \frac{\sum T_t \sqrt{\frac{2pqg_c}{RT_t}} \Delta A}{\sum \sqrt{\frac{2pqg_c}{RT_t}} \Delta A}$$

or, since static pressure is considered constant across the duct,

$$T_m = \frac{\sum \sqrt{q T_t} \Delta A}{\sum \sqrt{\frac{q}{T_t}} \Delta A} \quad (3)$$

The dynamic-pressure and total-temperature values measured by this survey method can be substituted directly into equation (3) to obtain the mean temperatures from which combustion efficiency is calculated.

3532

Total-Pressure Loss

The loss in total pressure of a combustion system is the difference between the total pressure of the air entering the system and that of the gases leaving it. A common dimensionless pressure-loss ratio is $\Delta P_t/q_1$, where q_1 is the inlet dynamic pressure. This pressure ratio is a function of the density ratio across the combustor (see ref. 13). Another common pressure-loss parameter is the ratio of pressure loss to inlet total pressure $\Delta P_t/P_{t,1}$ used, for example, in analytical studies in reference 14.

As with temperature determinations, it is necessary to traverse the gas streams to obtain mean total-pressure values. The expression for mass-weighted total pressure (i.e., the total pressure of a uniform stream having the same mass flow and kinetic energy as the actual exhaust gases) is written (ref. 1) as follows:

$$P_m = \frac{\sum P_t \left(\frac{W}{A}\right) \Delta A}{\sum \left(\frac{W}{A}\right) \Delta A} = P + \frac{\sum \sqrt{\frac{q^3}{T_t}} \Delta A}{\sum \sqrt{\frac{q}{T_t}} \Delta A} \quad (4)$$

Other weighting methods involving effective values of static pressure for a one-dimensional flow assumption are given in reference 15.

RESULTS AND DISCUSSION

In the following section, results of a survey taken by the polar-coordinate survey method are presented. The survey section was placed at the exhaust of a turbojet-combustor installation operated at average exhaust-gas conditions of 2000° F and 750 feet per second.

For the illustrative example run reported here, combustor-inlet conditions were as follows:

Total temperature, °F	840
Total pressure, lb/sq in. abs	25.0
Reference air velocity based upon inlet-air density and maximum combustor area, ft/sec	200
JP-4 fuel heating value, Btu/lb	18,700
Fuel-air ratio	0.018

Profiles and Contour Maps

Data recorded for this survey example are presented in figure 4, which shows temperature-position traces (fig. 4(a)) and dynamic-pressure-position traces (fig. 4(b)). Contour maps constructed from these data are given in figure 5. On these maps, lines of equal temperature and dynamic pressure are plotted directly on a scale drawing of the quarter-annular exhaust duct, graduated in polar coordinates.

Temperature contour maps. - Total-temperature patterns are presented in figure 5(a). Temperature points along the five circumferential paths that were surveyed were placed on the map, and then the equal temperature contour lines were interpolated. The isotherms with the most characteristic curvature, such as the 2300° and the 1800° curves, are constructed first; and intermediate temperature lines are then drawn between them, since the isothermal curves must not intersect. With a little practice, precise patterns can be drawn.

The temperature contour map presents radial and circumferential exhaust profiles in one plot, and it is therefore a useful means of studying the influence of combustor design upon exhaust temperature patterns. Relatively hot or cold regions shown on the map can often be linked to air-entry-hole or -slot patterns in the combustor. Design changes for altered temperature profiles then may be made with the contour map as a guide. The marked cooling effect of the duct side walls is also evident in the temperature contour map in figure 5(a). These side walls would not be present in a full annular exhaust duct, and the circumferential temperature gradients would be reduced.

Radial gradients at any circumferential position, to correspond to turbine blade locations, are constructed by cross plots taken at the desired circumferential station. In figure 5(a), as an illustration, a radial profile at 10° to the left of the centerline would show a peak temperature of over 2600° at the center, an outer-wall (tip) temperature of about 2400°, and an inner-wall (hub) temperature of about 2200°. An over-all average radial profile may also be obtained from the weighted mean circumferential temperatures.

Pressure, velocity, and flow contour maps. - The dynamic-pressure patterns presented in figure 5(b) are constructed in the same manner as the temperature patterns. The highest dynamic pressures are found in the lower corners, while the lowest dynamic pressures are at the upper left corner. For incompressible flow, dynamic pressure is directly proportional to the square root of Mach number (appendix B); and, accordingly, Mach number values corresponding to each isobar value are also shown in figure 5(b). Dynamic-pressure values of 1.4 and 1.9 pounds per square inch describe most of the flow area, corresponding to a Mach number range of 0.32 to 0.37, sufficiently low to justify the incompressible-flow assumption. With this combustor configuration, pressures and Mach numbers are greatest at the lower portion of the duct. In contrast to the temperature contours, circumferential pressure gradients are small.

A velocity pattern map, calculated from the total-temperature and dynamic-pressure data by the equation given in appendix B, is shown in figure 6(a). The influence of temperature is seen from a comparison of the dynamic-pressure pattern in figure 5(b) and the velocity pattern in figure 6(a). The highest velocities are found close to the lower radius, corresponding to the location of the highest dynamic pressures; circumferentially, however, the highest velocities are near the centerline, the region where the highest temperature are found.

Mass-flow patterns for this example are shown in figure 6(b). The equation for mass flow as an incompressible-flow function of temperature and dynamic pressure is derived in appendix B. Temperature has an inverse influence on mass flow, and the highest mass flows thus occur at the low-temperature - high-dynamic-pressure region along the lower side walls.

Combustion Efficiency

The weighted mean temperature, calculated in accordance with equation (3) for the run illustrated in this report, was 1967° F. For the inlet conditions cited previously, combustion efficiency, computed by the method of reference 12, was 96.0 percent.

As discussed previously, the combustion-efficiency calculation is based upon a representative mean exhaust temperature. The determination of an accurate mean temperature rests upon two factors: (1) a complete survey of the exhaust duct, and (2) proper weighting of the local measurements.

Completeness of survey. - Ordinary fixed thermocouple rakes have proved satisfactory for complete surveys at moderate temperature conditions with small temperature and pressure gradients (ref. 3). On the

3532 other hand, for the typical high-temperature patterns of figure 5(a), there are wide variations in temperature. It is evident that, if stationary rakes are used, a large number of elements is required because of the steep gradients. At extreme conditions a placement of one thermocouple per square inch of cross section, or nearly 60 thermocouples for this duct, is advised in the literature (see the discussion following ref. 3, pp. 333-334). With half this number of thermocouples, the maximum that could be physically accommodated at one cross-sectional plane in this duct, a symmetrical placement of thermocouples gave average temperature readings that were 150° too high for the example cited here. This high average temperature is due to an incomplete survey, particularly at regions near the side walls.

2-20 The polar-coordinate survey method furnishes a means of obtaining these complete surveys. There is negligible disturbance of the flow by the measuring elements, because the method employs only a single probe. For the example cited here, surveys at five radial positions were sufficient. When desired, however, additional circumferential sweeps for more complete coverage could be included without any further instrumentation or area blockage.

Weighting methods. - The second factor in temperature measurement is the requirement of proper weighting methods. Mean temperatures are determined by mass-weighting as shown by equation (3), written for incompressible flow and constant static pressure. The mass-weighted temperature shown in table I was calculated by using 45 equally spaced temperature and dynamic-pressure points on each circumferential survey from the original data shown in figure 4. This method is ordinarily most convenient, although further precision could be obtained by planimeter integration.

In practice, the mass-weighting procedure is rarely used. Mean temperatures are generally expressed as area averages. If the local temperature points represent equal area increments, the area-average temperature is simply an arithmetic average of the individual temperature points. Even where the mass-flow distribution is not uniform, an area-average temperature may be acceptable. For example, the area-average temperature for the run illustrated here based upon the same number of points as the mass-weighted temperature is 1993° F, 26° higher than the mass-weighted temperature; and the calculated combustion efficiency is 2.4 percentage points higher. Mass-weighted and area-average temperatures are compared at each circumferential survey radius in table I.

The comparison shows that, while the compromises involved in using an area-average temperature are recognized, the difference between this average and the correct mean temperature may be small. The mass-flow

contours in figure 6(b) suggest that this discrepancy should be greater, but probably compensating inequalities in the mass-flow distribution cancel out. No criterion can be offered here as to whether mass weighting is necessary in a given case.

Total-Pressure Loss

The weighted mean total pressure, calculated in accordance with equation (4), was 23.2 pounds per square inch absolute for the run illustrated in this report. Inlet total pressure was 25.0 pounds per square inch; thus, the total-pressure loss was 1.8 pounds per square inch, or 7.2 percent of the inlet total pressure.

The previous discussion of the need for a complete temperature survey and proper weighting of temperature data also applies to pressure measurements. Because total-pressure gradients are not as great as temperature gradients, the completeness of the survey or the method of weighting is not as important for pressure measurements. The total pressure for this run calculated by area-averaging was identical to the value obtained by mass-weighting. Pressure values at each radius by the two methods may be compared in table I.

Total-pressure loss could also be recorded directly in this survey method by connecting a combustor-inlet total-pressure tube and the exhaust-probe total-pressure tube to the pressure transducer. This method is most suitable where pressure loss is of prime importance rather than combustion efficiency or velocity profiles. On the other hand, in many cases as is illustrated here, recording dynamic pressure directly rather than pressure loss is preferred for convenience in mass-weighting and velocity calculations.

CONCLUDING REMARKS

A survey method for determining jet-engine combustor performance has been described. The method employs an automatic polar-coordinate traversing system that actuates a combined temperature and pressure probe for surveys of turbojet-combustor-exhaust ducts. Computation techniques are given for performance calculations from the survey data. The method furnishes a complete temperature and pressure survey and a means of calculating mass-weighted or area-average temperatures and pressures for evaluating combustion efficiency and pressure loss. A single movable probe assures a minimum disturbance of the exhaust-duct flow patterns.

An example was given to illustrate the survey method. The choice of the probe, survey cross section, and traversing path, however, is not limited to the high-temperature application cited in this report. The system may be used to actuate static-pressure tubes, exhaust-gas sampling tubes, anemometers, and other sensing devices. The traversing path may be rearranged to include circumferential sweeps at any desired number of radii; or, conversely, the positioning control can be rearranged for radial traverses at predetermined circumferential locations.

Lewis Flight Propulsion Laboratory
National Advisory Committee for Aeronautics
Cleveland, Ohio, July 19, 1955

2252

CG-2 back

APPENDIX A

AUTOMATIC POSITIONING CONTROL

The probe travel of circumferential sweeps at predetermined radii, shown in figure 3, is governed by an automatic controller. Angular and radial motion alternate with one drive energized at a time as determined by the control circuit (fig. 7).

The radial position is controlled by a self-balancing Wheatstone bridge with a closed-loop servomechanism. The ratio of resistance between two arms of the bridge reflects a specific probe position, since a precision multiturn potentiometer (R14) geared directly to the probe radial actuator provides this resistance ratio. The ratio of the remaining two resistive arms is one of five predetermined ratios, representing a radial probe position, selected through a stepping switch (relay 6 and resistors R1 to R6). If the probe is at another radius, the bridge unbalance voltage is amplified and powers the actuator motor through output relay 1 or 2 to drive the bridge to balance.

Limit switches (Sw. 3 and 4) control the angular-drive motor through relays 3 and 4, which determine the direction of angular drive. Relay 4 also sends a pulse of current through either condenser C1 or C2 at the end of each angular sweep that steps relay 6, driving the probe to a new radial position. During radial drive, power is removed from the angular-drive motor by relay 1 or 2. After the last arc of a survey is completed, relay 5 stops the angular motor. The next survey retraces this motion in a reverse direction.

A probe is installed in such a way that the tip extends to the proper radius for a given position of the radial-drive lead screw. To simplify installation of replacement probes, switch 1 is switched to "manual." Resistor R7 is set to a ratio of resistance such that the probe actuator drives the probe until its tip just touches the outer duct wall. When a new probe is installed with the radial actuator so positioned, the relation between the probe tip and the radial-drive lead screw is correct.

The photograph (fig. 8) shows the arrangement of the necessary actuating elements at the survey duct section. The angular-drive gear, motor, and potentiometer for position transmitting are mounted behind the metal plate at the lower left. Projections on the angular-drive hub contact limit switches, one of which is shown in figure 8, at the end of the angular travel. This hub is held in place by two spring-loaded bearing blocks that ensure good contact between the hub and the cushion block above it. The radial-drive actuator and motor are also

shown in figure 8, and the precision potentiometer for probe-radius control (R14) lies behind the radial-drive motor. The drive mechanisms are ordinarily covered by a radiation hood (not shown in fig. 8) for protection from heat damage.

3532

APPENDIX B

CALCULATION OF MACH NUMBER, MASS FLOW, AND VELOCITY FROM
TEMPERATURE AND PRESSURE

Compressible Case

For the rigorous case where flows are considered compressible, Mach number, mass flow, and velocity are derived from the measured values of total temperature, static pressure, and the difference between total and static pressure, determined across the duct by the survey probe.

The relation between total and static pressure and Mach number is

$$\frac{P_t}{p} = \left(1 + \frac{\gamma-1}{2} M^2\right)^{\frac{\gamma}{\gamma-1}} \quad (B1)$$

When equation (B1) is solved for Mach number, it is found that

$$M = \sqrt{\frac{2}{\gamma-1} \left\{ \left[\frac{(P_t - p) + p}{p} \right]^{\frac{\gamma-1}{\gamma}} - 1 \right\}} \quad (B2)$$

Mass flow is calculated by means of the continuity relation in terms of Mach number, static pressure, and total temperature. Thus,

$$\frac{w}{A} = pM \sqrt{\frac{\gamma g_c \left(1 + \frac{\gamma-1}{2} M^2\right)}{RT_t}} \quad (B3)$$

From a substitution of equations (B1) and (B2) into equation (B3),

$$\frac{w}{A} = p \sqrt{\frac{2\gamma g_c}{(\gamma-1)RT_t} \left\{ \left[\frac{(P_t - p) + p}{p} \right]^{\frac{2(\gamma-1)}{\gamma}} - \left[\frac{(P_t - p) + p}{p} \right]^{\frac{\gamma-1}{\gamma}} \right\}} \quad (B4)$$

Velocity is expressed in terms of Mach number; and, thus, from a substitution of equation (B2) for Mach number,

$$V = \sqrt{\frac{2\gamma g_c RT_t}{\gamma-1} \left\{ 1 - \left[\frac{(P_t - p) + p}{p} \right]^{\frac{\gamma}{\gamma-1}} \right\}} \quad (B5)$$

These equations show how Mach number, velocity, and mass-flow quantities are related to the measured temperature and pressure values. For expedience in calculation, compressible flow charts such as those in reference 16 can be used.

Incompressible Case

With the assumption of incompressible flow, the measured difference between total and static pressure is equivalent to the dynamic pressure. Thus, Mach number may be expressed in terms of dynamic pressure as

$$M = \sqrt{\frac{2q}{\gamma p}} \quad (B6)$$

or Mach number is directly proportional to the square root of dynamic pressure for constant specific-heat ratio and static pressure across the duct. For a specific-heat ratio of 1.30, equation (B6) at Mach number levels of 0.4 gives a Mach number value about 2 percent higher than the more exact value calculated from equation (B2).

The mass-flow relation is derived from the continuity equation expressed in terms of dynamic pressure, static pressure, and total temperature, which is assumed equivalent to static temperature. Thus,

$$\frac{w}{A} = \sqrt{\frac{2g_c p q}{RT_t}} \quad (B7)$$

or mass flow per unit area is proportional to the square root of the ratio of dynamic pressure to total temperature. The substitution of total temperature for static temperature introduces an error of less than 3 percent at Mach numbers of 0.4 for a specific-heat ratio of 1.30.

Similarly, velocity is expressed in terms of dynamic pressure, static pressure, and total pressure by

$$V = \sqrt{\frac{2g_c RT_t q}{p}} \quad (B8)$$

Velocity is therefore proportional to the square root of the product of dynamic pressure and temperature.

REFERENCES

1. Watson, E. A., and Clarke, J. S.: Combustion and Combustion Equipment for Aero Gas Turbines. Jour. Inst. Fuel, vol. XXI, no. 116, Oct. 1947, pp. 2-34.

2. Probert, R. P., and Singham, J. R.: The Measurements of Gas Temperatures in Turbine Engines. Jour. Sci. Instr., vol. 23, no. 4, Apr. 1946, pp. 72-77.
3. Olson, Walter T., and Bernardo, Everett: Temperature Measurements and Combustion Efficiency in Combustors for Gas-Turbine Engines. Trans. A.S.M.E., vol. 70, no. 4, May 1948, pp. 329-333.
4. Dunning, J. E. P.: Note on a Suggested Method of Measurement of High Temperatures in Gases Moving with High Velocity, with Particular Reference to Low Pressure Conditions. Tech. Note Aero. 1872, British R.A.E., Feb. 1947.
5. Lloyd, Peter: Determination of Gas-Turbine Combustion-Chamber Efficiency by Chemical Means. Trans. A.S.M.E., vol. 70, no. 4, May 1948, pp. 335-341.
6. Allen, Sydney, and Hamm, J. R.: A Pyrometer for Measuring Total Temperatures in Low-Density Gas Streams. Trans. A.S.M.E., vol. 72, no. 6, Aug. 1950, pp. 851-858.
7. Lalos, George T.: A Sonic-Flow Pyrometer for Measuring Gas Temperatures. Jour. Res. Nat. Bur. Standards, vol. 47, no. 3, Sept. 1951, pp. 179-190.
8. Hottel, H. C., and Kalitinsky, A.: Temperature Measurements in High-Velocity Air Streams. Jour. Appl. Mech., vol. 12, no. 1, Mar. 1945, pp. A25-A32.
9. Scadron, Marvin D., Warshawsky, Isidore, and Gettelman, Clarence C.: Thermocouples for Jet-Engine Gas Temperature Measurement. Proc. Instr. Soc. Am., Paper No. 52-12-3, vol. 7, 1952, pp. 142-148.
10. Scadron, Marvin D., and Warshawsky, Isidore: Experimental Determination of Time Constants and Nusselt Numbers for Bare-Wire Thermocouples in High-Velocity Air Streams and Analytic Approximation of Conduction and Radiation Errors. NACA TN 2599, 1952.
11. Nichols, J. B.: An Energy Basis for Comparison of Performance of Combustion Chambers. Trans. A.S.M.E., vol. 75, Jan. 1953, pp. 29-33, discussion, p. 33.
12. Turner, L. Richard, and Bogart, Donald: Constant-Pressure Combustion Charts Including Effects of Diluent Addition. NACA Rep. 937, 1949. (Supersedes NACA TN's 1086 and 1655.)
13. Childs, J. Howard, McCafferty, Richard J., and Surine, Oakley, W.: Effect of Combustor-Inlet Conditions on Performance of an Annular Turbojet Combustor. NACA Rep. 881, 1947. (Supersedes NACA TN 1357.)

14. Pinkel, I. Irving, and Shames, Harold: Analysis of Jet-Propulsion-Engine Combustion-Chamber Pressure Losses. NACA Rep. 880, 1947. (Supersedes NACA TN 1180.)
15. Wyatt, DeMarquis D.: Analysis of Errors Introduced by Several Methods of Weighting Nonuniform Duct Flows. NACA TN 3400, 1955.
16. Turner, L. Richard, Addie, Albert N., and Zimmerman, Richard H.: Charts for the Analysis of One-Dimensional Steady Compressible Flow. NACA TN 1419, 1948.

3532

CG-3

TABLE I. - COMBUSTOR PERFORMANCE FOR ILLUSTRATED RUN

Circumferential survey path (fig. 3)	Exhaust temperature, °F		Exhaust total pressure, lb/sq in. abs	
	Mass-weighted average	Area average	Mass-weighted average	Area average
Radius 1	1875	1872	22.8	22.8
Radius 2	1963	1996	23.0	23.0
Radius 3	2029	2056	23.2	23.2
Radius 4	1999	2040	23.5	23.5
Radius 5	1970	2000	23.4	23.4
Over-all average	1967	1993	23.2	23.2
Combustion efficiency, percent	96.0	98.4		
Total-pressure loss, percent of inlet total pressure of 25.0 lb/sq in. abs			7.2	7.2

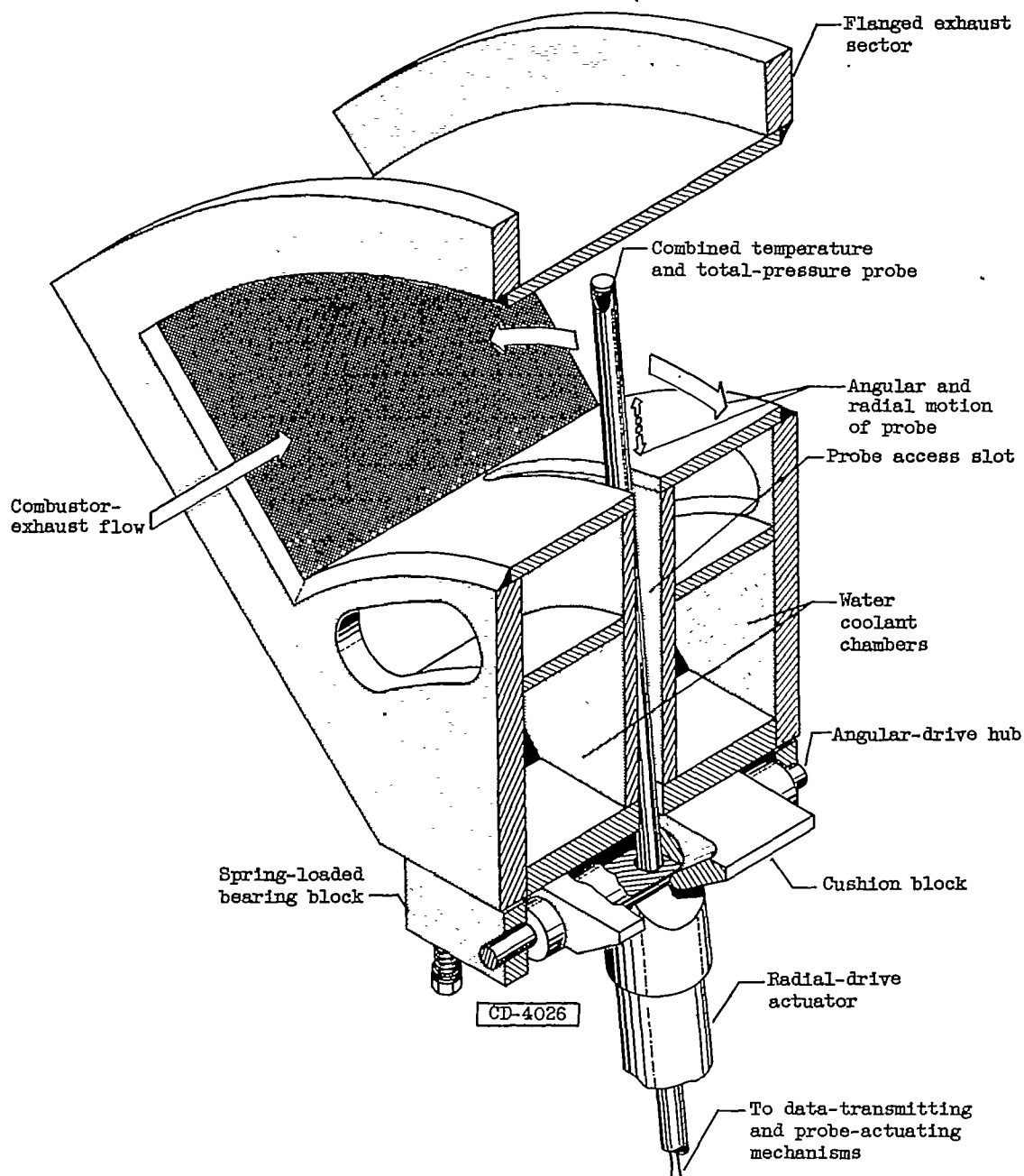


Figure 1. - Cutaway view of polar-coordinate survey section with probe in place.

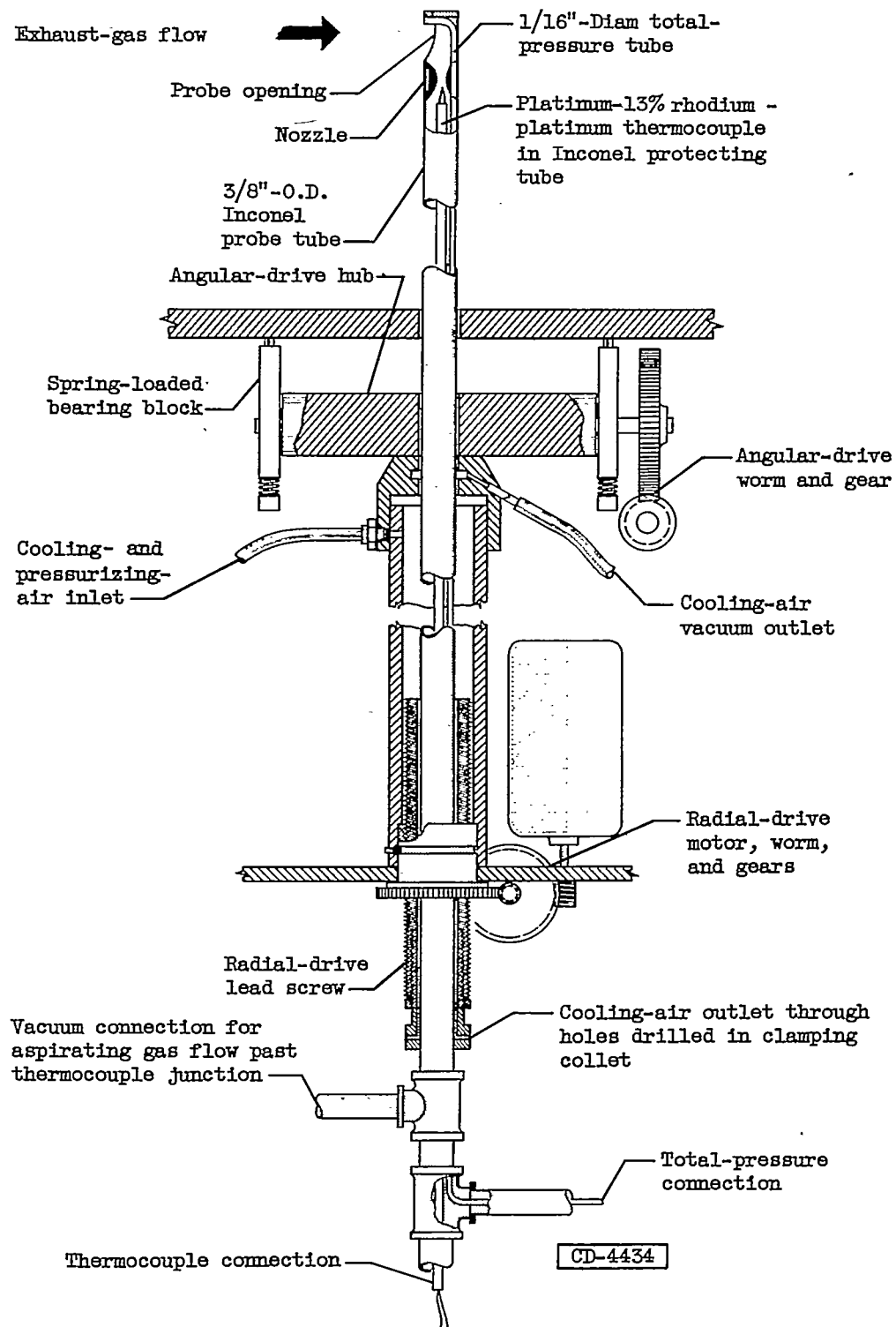


Figure 2. - Cross-sectional view of probe installation.

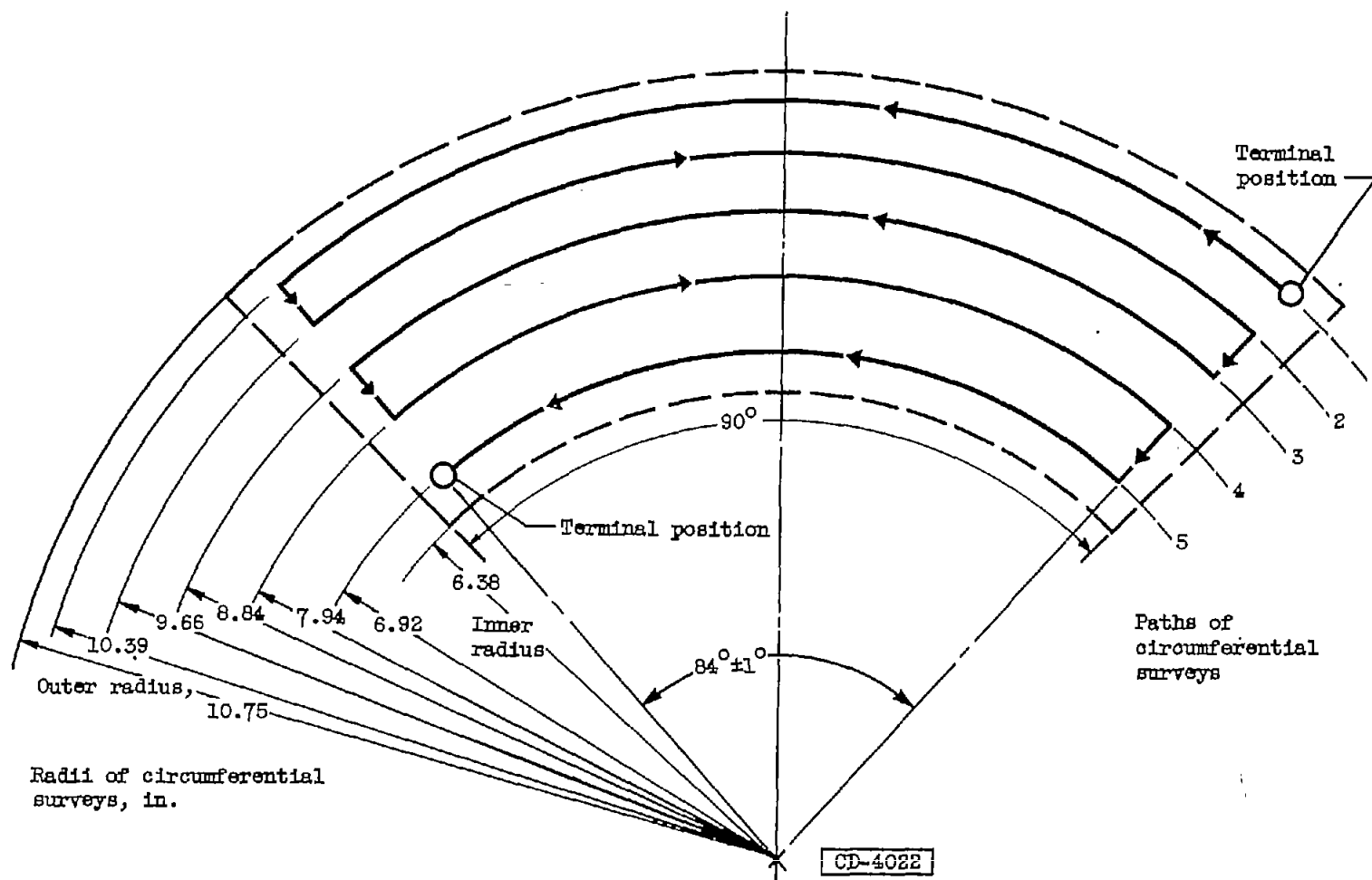
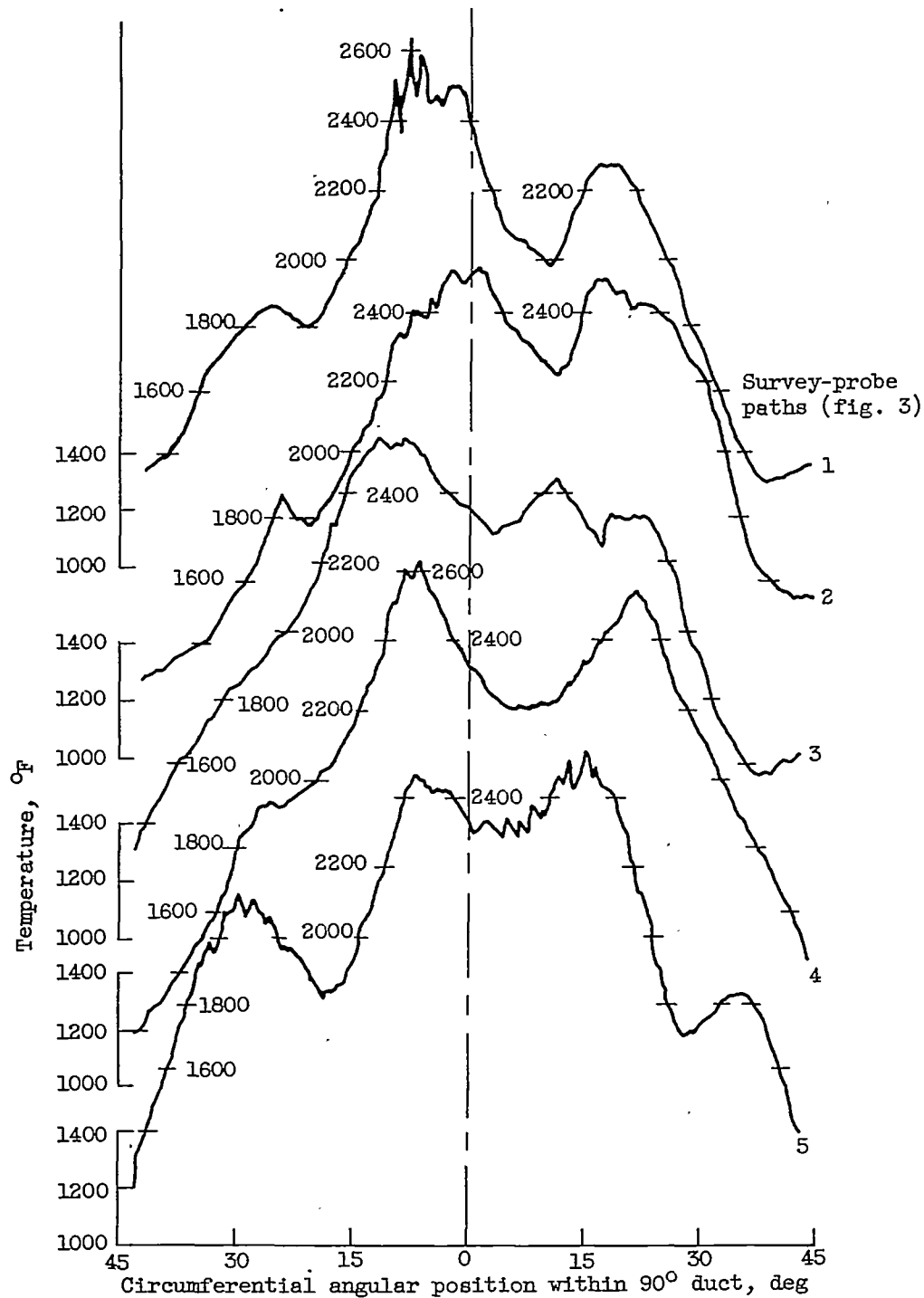


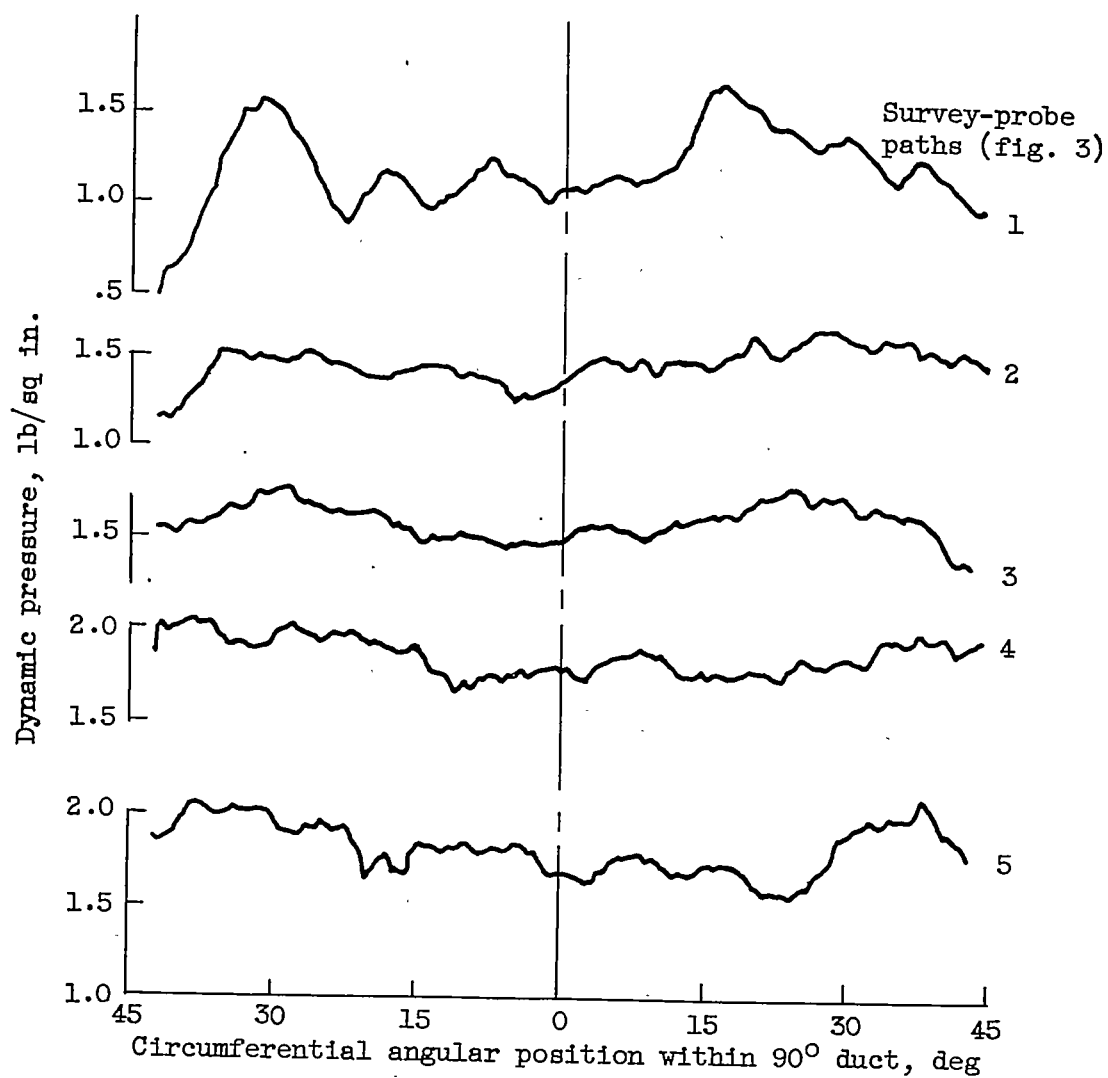
Figure 3. - Path surveyed by probe tip across combustor-exhaust section, showing circumferential sweeps at five radii at centers of equal area.



(a) Total-temperature survey.

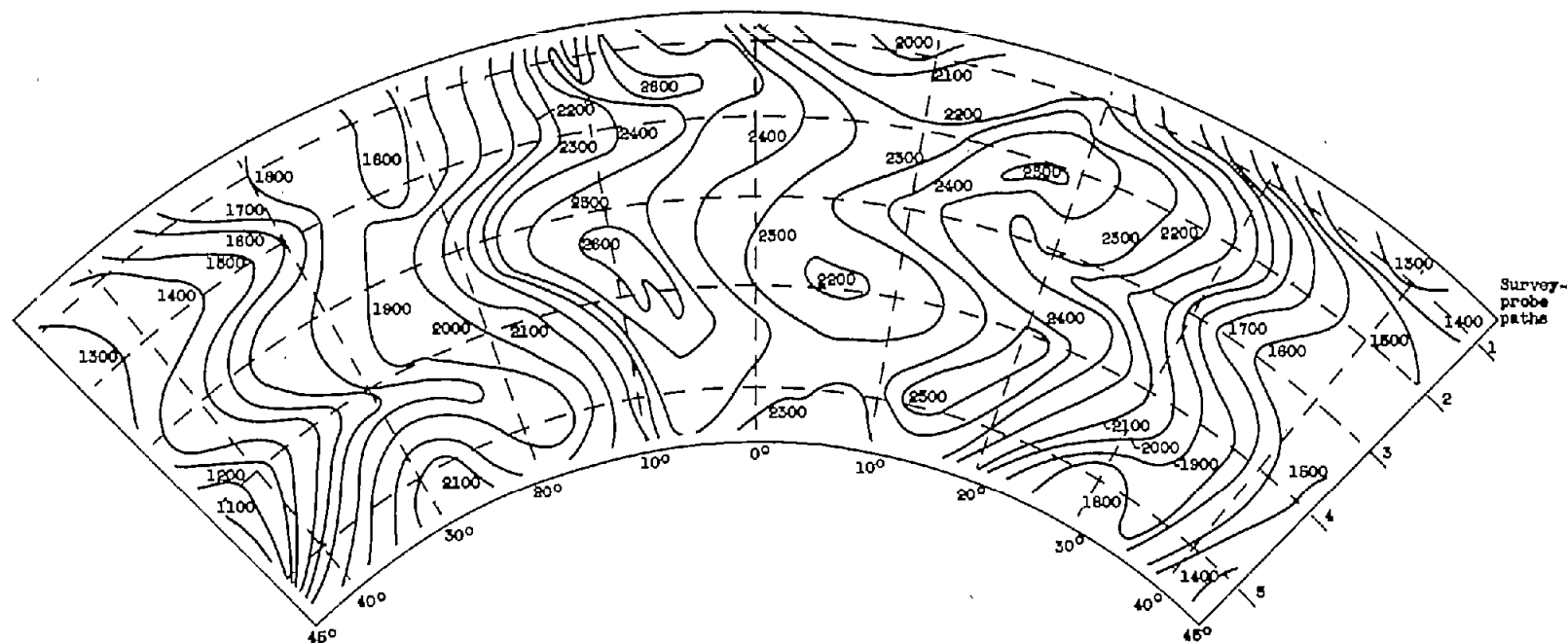
Figure 4. - Total-temperature and dynamic-pressure survey records for typical combustor-exhaust survey.

3532



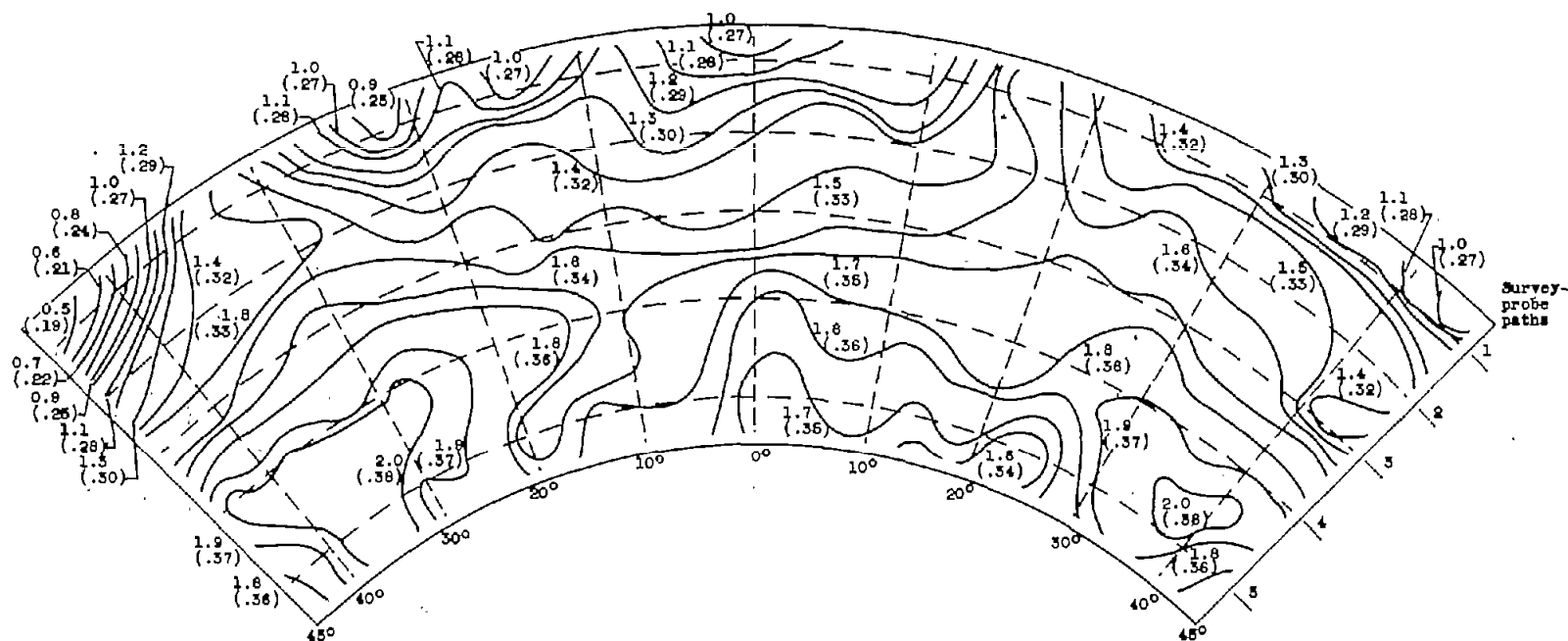
(b) Dynamic-pressure survey.

Figure 4. - Concluded. Total-temperature and dynamic-pressure survey records for typical combustor-exhaust survey.



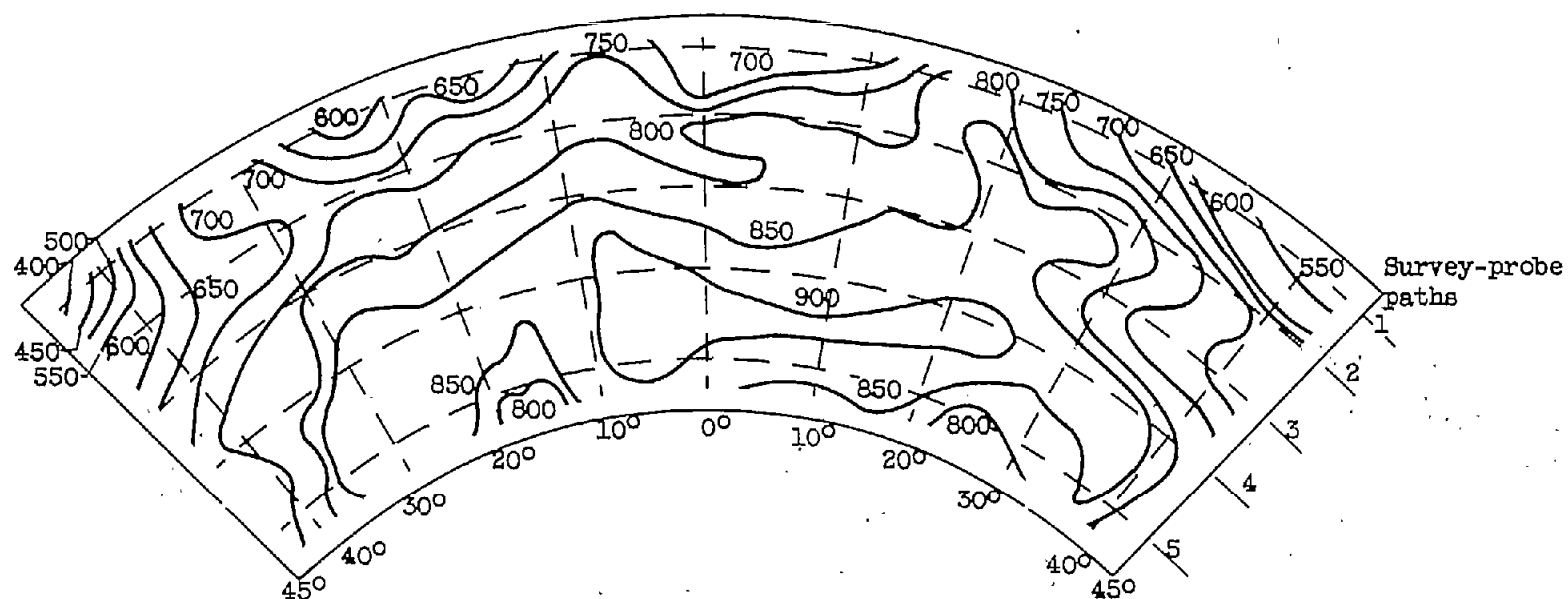
(a) Temperature patterns, °F.

Figure 5. - Contour patterns for combustor-exhaust survey derived from recorded circumferential traces of temperature and pressure.



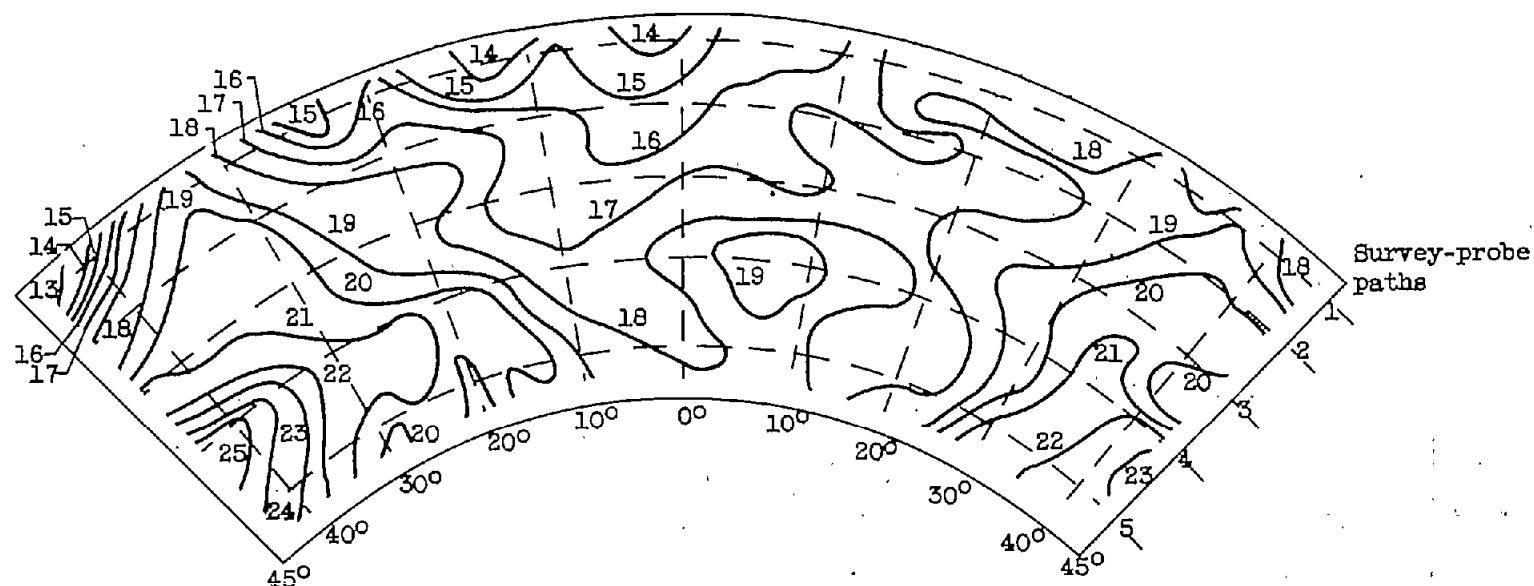
(b) Dynamic-pressure patterns, pounds per square inch. (Corresponding Mach number values in parentheses.)

Figure 5. - Concluded. Contour patterns for combustor-exhaust survey derived from recorded circumferential traces of temperature and pressure.



(a) Velocity contours, feet per second.

Figure 6. - Contour maps of calculated flow quantities, derived from combustor-exhaust survey of temperature and pressure.



(b). Contours of mass flow per unit area, pounds per square foot per second.

Figure 6. - Concluded. Contour maps of calculated flow quantities, derived from combustor-exhaust survey of temperature and pressure.

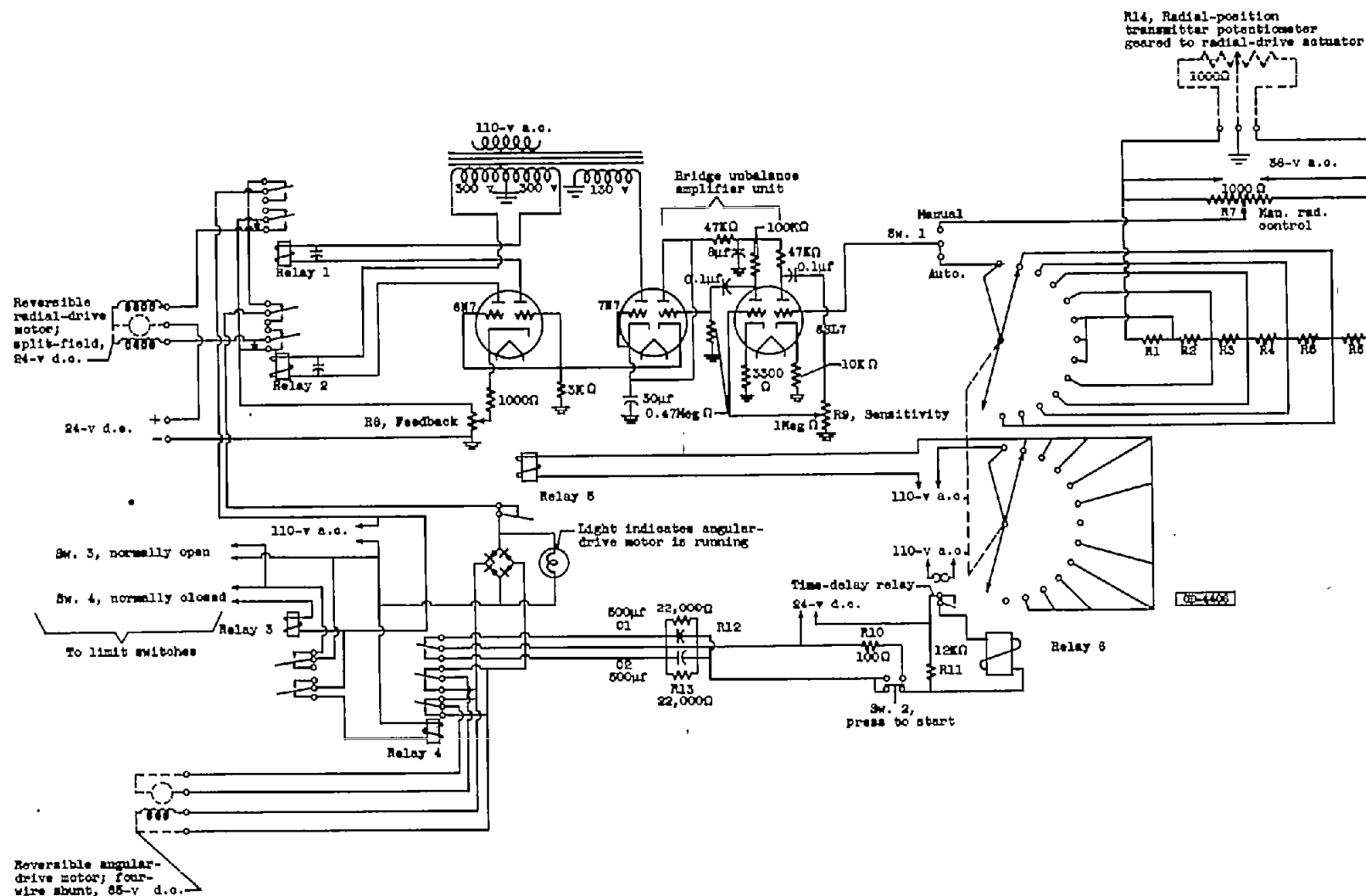


Figure 7. - Circuit diagram for automatic positioning control.

3532

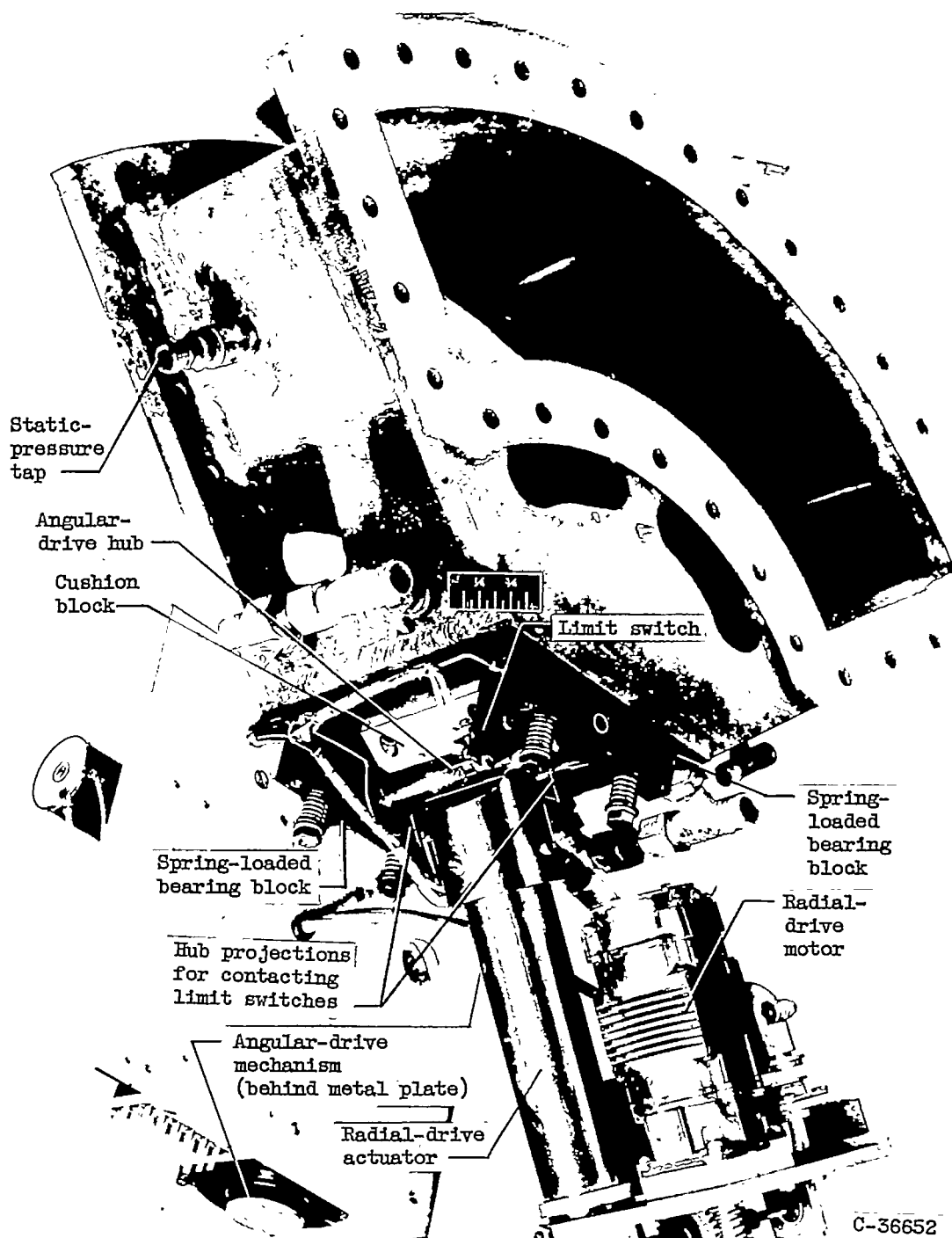


Figure 8. - Photograph of polar-coordinate survey section.